Supplement prepared for Biogeosciences
Date: 15 April 2010

Supplement to 'Regional carbon dioxide and energy fluxes from airborne observations using flight-path segmentation based on landscape characteristics'

O. S. Vellinga[1,3], B. Gioli[2], J. A. Elbers[1], A. A. M. Holtslag[3], P. Kabat[1], and R. W. A. Hutjes[1]

[1]Wageningen University, Earth-System Science & Climate-Change Group, Wageningen, the Netherlands
[2]Institute of Biometeorology, IBIMET-CNR, Florence, Italy
[3]Wageningen University, Meteorology & Air-Quality Group, Wageningen, the Netherlands

1 Introduction

In the main article, we stated that we performed our airborne measurements above the so-called 'local' blending height, when flying on average 82 m (σ = 14 m) above the ground. The analysis in the following section supports this statement.

Next to this, we stated in the main article that flux divergence between surface and the flight level, at which we have flown our flight tracks, probably led to a small underestimation of our airborne regional fluxes. The analysis in the last section supports this statement.

2 Blending Height

In a heterogeneous landscape with heterogeneities occurring at length scales less than approx. 10 km (i.e., type-A heterogeneity or meso-heterogeneity; Shuttleworth, 1988; Mahrt, 2000), internal boundary layers merge due to the turbulent mixing. The influence of individual surface elements, like individual agricultural fields, vanishes above this (local) blending height. The height mainly depends on the spatial scale of the heterogeneities and — to a lesser extend — on atmospheric stability. We used the model by Wood et al. (1991), which includes both the spatial scale and the atmospheric stability, to calculate the blending height z_b:

$$z_b = 2 \times \left(\frac{u_*}{\overline{U}}\right)^2 \times L_H, \tag{1}$$

where L_H is the average length of the surface heterogeneities; u_* is the friction velocity; and $\overline{U}$ is the wind speed. The latter two are both above the blending height and the ratio of the two is related to the atmospheric instability. This ratio becomes larger with increasingly convective conditions or increased mechanical turbulence. A larger ratio, therefore, means an increase in blending height.

In a heterogeneous landscape with heterogeneities occurring at length scales of about 10 km and greater (i.e., type B as in Shuttleworth, 1988), the (regional) blending height is less easy to define as also mesoscale processes may come into play. However, it is safe to assume that this regional blending height is at least an order of magnitude larger than the local one.

We estimated the length scale of the heterogeneities in each segment by simply counting the number of separate (2 D) fields, forests and built-up areas directly under the flight track, while neglecting line elements, like roads, hedges, etc. The total number of elements in a segment was then divided by its length. Table 1 and 2 shows that the average field size in our domain is small and varies from about 100 m in segment 5 to about 350 m in segment 6, while in most segments is around 150 m. First-order estimates already indicated, we would be flying above the local blending height. Thus, we simply used the aircraft observed wind speed and friction velocity directly in formula 1. This results in blending heights on average between 20–30 m, though incidentally, it reaches up to about 80 m in segment 12 during IOP 1.

This brief analysis shows that the flight levels, at which we have been flying, were well above the 'local' blending height and flux variations from individual fields were no longer recognisable in the measurements. Strictly speaking, formula 1 applies to a landscape heterogeneous in roughness only. However, a variant of the same formula for heat flux heterogeneities (Wood et al., 1991; Mahrt, 2000) applied to our data suggested even lower blending heights. On the other hand, we assume flight levels were well below the 'regional' blending height (relevant for type-B heterogeneity or macro-heterogeneity; Shuttleworth, 1988; Mahrt, 2000), thus, making sure that the differences between the segments generally do not become significantly convoluted.

Correspondence to: O. S. Vellinga
(olaf.vellinga@wur.nl)

Table 1. Average wind speed ($\overline{U}$), average friction velocity (u_*), estimated length scale (L_H) and estimated blending height (z_b) for each segment along average flight track for both IOPs during CERES '07.

Segment	Length km	Counts	L_H m	$\overline{U}$ m/s	u_* m/s	z_b m
3	14	94	146	2.6	0.75	24
4	35	289	119	2.6	0.70	17
5	15	151	99	2.3	0.50	10
6	13	35	357	2.6	0.61	41
7	30	244	123	1.6	0.54	29
8	5	31	155	1.8	0.53	28
9	24	161	149	2.4	0.52	15
10	16	101	156	2.6	0.53	13
11	20	104	194	2.3	0.64	29
12	12	73	163	1.9	0.97	84
Totals	182	1283				

Table 2. Same as Table 1, but now for IOP 2

Segment	Length km	Counts	L_H m	$\overline{U}$ m/s	u_* m/s	z_b m
3	14	94	146	n/a	n/a	n/a
4	35	289	119	3.0	0.88	20
5	15	151	99	2.8	0.75	15
6	13	35	357	2.7	0.79	60
7	30	244	123	3.6	0.82	13
8	5	31	155	3.2	0.60	11
9	24	161	149	3.0	0.89	27
10	16	101	156	3.2	0.89	24
11	20	104	194	3.5	0.81	21
12	12	73	163	3.9	0.67	10
Totals	182	1283				

3 Flux Divergence

3.1 Introduction

An experiment focussing on daytime flux divergence across the atmospheric boundary-layer was conducted during the CarboEurope-IP's Regional Experiment in the south-west of France (CERES '07) on September 13, 2007. The aim of the flux-divergence experiment was to observe how exchange of energy and carbon dioxide behaves at the surface and across the convective boundary-layer (CBL) by measuring fluxes with the eddy-covariance technique with two small environmental research aircrafts (SERAs) at the same time. It was carried out in collaboration with the Italian airborne team of IBIMET-CNR, who operates the same type of SERA as we are using (see main article for more details). Outcome of this experiment in the frame of the current work is to assess the surface representativeness of airborne flux-measurements taken at about 82 m above ground level (agl), in terms of vertical flux divergence and other disturbing factors.

Our flight strategy was to combine flights of both aircrafts measuring carbon and energy fluxes at the surface (about 85 m agl) and at several flight levels up to 90 % of the CBL-height during one day. Each flight was performed in the same manner: a vertical profile to find the top of the CBL, then followed by a number of equally spaced flight levels between the surface and the top of CBL, where at each flight level, a straight leg of 10 km was flown four times. Four flights have been carried out in this way, where the first and last flight were done by only one aircraft due to the shallow CBL-height. The reason to use two aircraft for the midday experiments was to reduce the total time required to complete all the legs, and thus to increase the degree of stationarity during each experiment. The experiment was carried out over the ground station 'Marmande' (MA, see Fig. 2 in main article) which was located directly under the vertically stacked flight legs to have flux measurements at ground level available.

3.2 Implementation

The first flight (See Table 3) was performed by the Italian airborne team with their aircraft, called I-RAWH, between 08:00 till 10:02 UTC. During the vertical profile, the CBL-height was found at about 450 m. This determined the first flight level to be at 400 m followed by two other levels at 250 m and 85 m, respectively. Second and third flight (See Table 4) were carried out simultaneously by both aircrafts between 10:30 and 12:03 UTC. This time, our aircraft, called PH-WUR, determined the CBL-height at about 600 m. This resulted in six flight levels of which we did the upper three levels at 550, 450 and 365 m and the Italian team flew the lower three flight legs at 275, 180 and 85 m. The fourth and final flight (See Table 5) took place between 14:27 and 16:31 UTC and was carried out by our aircraft alone. Due to time constrains, the number of flights per leg was changed. Results of this last flight are not shown here, because conditions are not relevant for this study as it has been carried out during late afternoon with a collapsing CBL.

Figure 1 depicts all flight periods (rectangular boxes) plotted over the diurnal cycle of surface fluxes measured by the

Table 3. Set-up of flux-divergence flight no. 1 conducted with the small environmental research aircraft (SERA) of IBIMET-CNR (I-RAWH)

Type of Measurement	UTC
Vertical profile (CBL top ≈450 m agl)	08:00
4 flight legs @ 400 m agl	08:10 – 08:40
4 flight legs @ 250 m agl	08:46 – 09:15
4 flight legs @ 85 m agl	09:20 – 10:02

Table 4. Same as Table 3, but now flight no. 2 and no. 3 conducted with I-RAWH and the SERA of Wageningen UR (PH-WUR)

Type of Measurement	UTC
Vertical profile (CBL top ≈600 m agl)	10:30
4 flight legs @ 275 m agl I-RAWH	10:49 – 11:11
4 flight legs @ 180 m agl I-RAWH	11:15 – 11:37
4 flight legs @ 85 m agl I-RAWH	11:40 – 12:02
4 flight legs @ 550 m agl PH-WUR	10:49 – 11:11
4 flight legs @ 450 m agl PH-WUR	11:14 – 11:37
4 flight legs @ 365 m agl PH-WUR	11:40 – 12:03
Vertical profile	

Table 5. Same as Table 3, but now flight no. 4 conducted with PH-WUR

Type of Measurement	UTC
Vertical profile	
4 flight legs @ 1750 m agl	14:27 – 14:55
3 flight legs @ 1180 m agl	15:02 – 15:21
3 flight legs @ 650 m agl	15:27 – 15:47
6 flight legs @ 85 m agl	15:54 – 16:31

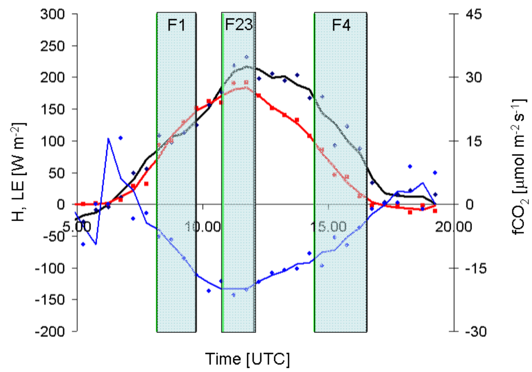

Fig. 1. Surface fluxes at ground station 'Marmande' during September 13, 2007, with flight periods of the flux-divergence experiment (F1, F2 + F3, F4) during CERES '07, where red line = sensible heat flux (H) and black line = latent heat flux (LE) both belonging to the left y-axis; blue line = carbon uptake (fCO_2)

ground station 'Marmande' during the experiment. From the figure, it becomes clear that all flights have been spread quite well over the day. The first and last flight (F1 and F4 in figure) took place when fluxes were, respectively, increasing and decreasing rapidly, while flight 2 and 3 were done right at the time of day that fluxes were around their maximum. During the first flight, sensible heat flux (H) increases from about 60 to about 145 $\mathrm{W/m^2}$, and latent heat flux (λE) increases at somewhat lower rate from about 75 to about 130 $\mathrm{W/m^2}$. The carbon uptake (fCO_2) increases during the same time period from about -4 to about $-16\,\mathrm{\mu mol/m^2/s}$. During the next two flights (F23 in figure), H and λE reach their maximum close to the end of the flights at about the same time at, respectively, about 180 and about 210 $\mathrm{W/m^2}$. The carbon uptake was directly at the start of the period at its maximum (approx. $-17\,\mathrm{\mu mol/m^2/s}$), while decreasing again close to the end of the flight periods to approx. $-16.5\,\mathrm{\mu mol/m^2/s}$. After the end of the second and third flight and before the start of the fourth flight, λE decreased at a lower rate than H, which results in larger λE during the final flight. During the final flight, both fluxes decreased at similar rates. At this period, λE decreased from about 165 to about 60 $\mathrm{W/m^2}$, while H decreased from about 100 to about 15 $\mathrm{W/m^2}$. Carbon uptake decreased from about -13.5 to about $-5\,\mathrm{\mu mol/m^2/s}$.

3.3 Results & Discussion

Figures 2, 3 and 4 show the results of the first flight performed by the Italian aircraft (I-RAWH), including the range of fluxes measured by the tower at station 'Marmande' during the time of flight. All ranges are large, indicating that fluxes were increasing with a high rate during the time of flight as shown in Fig. 1. With regard to the flux profiles, all fluxes decrease rapidly and more than linear with increasing height. Figure 2 shows the profile of carbon uptake, which decreases from on average $-11\,\mathrm{\mu mol/m^2/s}$ till nearly no flux close at the top of the CBL. The sensible heat flux (see Fig. 3) decreases with increasing height from on average 150 $\mathrm{W/m^2}$ at the ground to nearly zero close to the top of the CBL. The latent heat flux (see Fig. 4) decreases with increasing height from on average 110 $\mathrm{W/m^2}$ to nearly zero again close to the top of the boundary layer. Note the increase in variability (error bars) between the lowest and the middle flight level followed by a large decrease of it between the middle and the highest flight level.

These figures show fast changing conditions at the surface and entrainment fluxes are close to zero both for energy and carbon fluxes. Extrapolation of the flux profile by the aircraft to the ground level yields a value on the low end of the range observed by the tower at ground station 'Marmande'. This can be caused by different factors: (1) a difference in footprint areas between the two types of observations: an homogeneous maize field (with high uptake) for the tower versus a more patchy landscape (mostly maize fields with bare soils, green houses and roads) for the aircraft. This could justify the discrepancy between tower and airborne observations for fCO_2 and λE, but not for H; (2) since surface fluxes are rapidly changing, fluxes within CBL are also changing in response to the surface, but with a delay that takes into account the vertical mass and energy transfer; and (3) a higher flux-loss is present in the aircraft data, possibly related to low frequency contributions.

Figures 5, 6 and 7 show the results of the second and third flight, where the lower three flight levels were obtained by I-

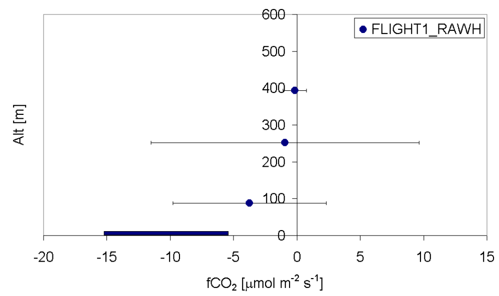

Fig. 2. Carbon-dioxide flux at different altitudes (circles) from flux-divergence flight no. 1 and its observed range at ground-site 'Marmande' during flight time (rectangular box)

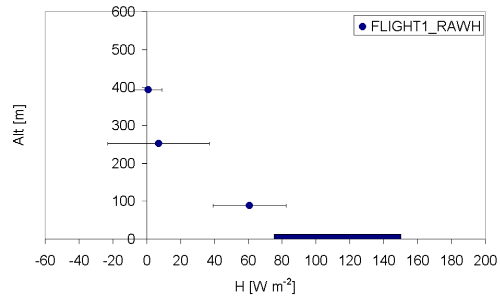

Fig. 3. Same as Fig. 2, but now for sensible heat flux (H).

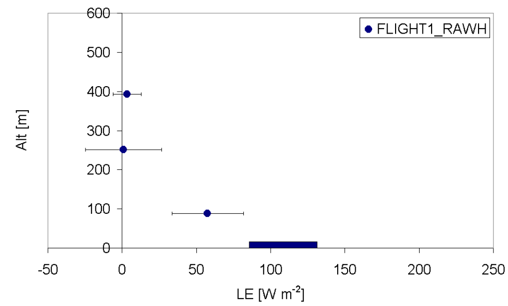

Fig. 4. Same as Fig. 2, but now for latent heat flux (LE).

RAWH and the upper three by PH-WUR. Note that the range of fluxes measured by the tower at station 'Marmande' is much smaller now, indicating that fluxes were at their maximum during the time of both flights as shown in Fig. 1. Here, all boundary-layer fluxes clearly decrease linearly with increasing height, compared to the first flight, with a clear offset between the fluxes of both aircrafts. Flux magnitudes appear lower for I-RAWH compared, when linearly extrapolating down the flux profile of the upper levels measured by PH-WUR. In case of fCO_2 (see Fig. 5), the highest flight level (T0 in figure) of the Italian aircraft is about $-5\,\mu\mathrm{mol/m^2/s}$, while the lowest level (T2) of our aircraft observed about $-7\,\mu\mathrm{mol/m^2/s}$. For H (see Fig. 6), the jump is less strong, where I-RAWH observed about $32\,\mathrm{W/m^2}$ at flight level T0 and PH-WUR measured about $34\,\mathrm{W/m^2}$ at level T2. However, the largest jump is found for λE (see Fig. 7) between both flight levels with approx. $55\,\mathrm{W/m^2}$ at level T0 and approx. $115\,\mathrm{W/m^2}$ at T2. In addition, for fCO_2 and H, large jumps can be found between the lowest flight level at $85\,\mathrm{m}$ (T2) and the ground station. Note that variability in these observations is large and they could contribute to observed discrepancy in mean values.

Since the two aircrafts were previously inter-calibrated and compared and no systematic difference in fluxes emerged, our explanation of this behaviour is that transients between different levels play an important role. Our hypothesis is that, while at the surface, fluxes are not changing much during flight time due to midday levelling of radiation, fluxes within the CBL are still growing. Testing this hypothesis would require a fully coupled CBL modelling framework, which we were not able to do so. We tested it by simply enhancing the fluxes measured earlier by an empirical factor: Choosing a factor of 1.3 (i.e., 30 % enhancement) for flights at time T0 (approx. one hour before T2) and 1.15 (i.e., 15 % enhancement) for flights at time T1 (approx. half hour before T2), we obtain flux profiles shown in figure 8, 9 and 10. The resulting linear relations are more robust for fCO_2 (see Fig. 8) and H (see Fig. 9), but not completely for λE (see Fig. 10). This is not an exhaustive analysis of such a complex topic, but it can confirm that a time shift of observations plays an important role (see also Bange et al., 2006).

Extrapolation of the linear flux profiles to the surface typically yields to values lower then measured from the tower, confirming what was found for the first flight. In other words, for H, $\simeq$180 $\mathrm{W/m^2}$ was measured at the tower and $\simeq$120 $\mathrm{W/m^2}$ was observed at about 85 m by the aircraft. Extrapolation of the flux profile to ground, yields $\simeq$140W/m^2. This possible underestimation of surface fluxes may in part be contributed by vertical flux divergence, and in part by flux-loss associated to airborne eddy covariance or transient effects, which means that divergence might be accounted for $\sim$20 $\mathrm{W/m^2}$ and $\sim$40 $\mathrm{W/m^2}$ for other factors. In case of fCO_2, tower observation was $\simeq -20\,\mu\mathrm{mol/m^2/s}$, while at about $85\,\mathrm{m}$ the aircraft observed $\simeq -12\,\mu\mathrm{mol/m^2/s}$. Extrapolation of the flux profile to the ground results in $\simeq -14\,\mu\mathrm{mol/m^2/s}$. Here, divergence might be accounted for $\sim$2 $\mu\mathrm{mol/m^2/s}$ and other factors for $\sim$6 $\mu\mathrm{mol/m^2/s}$. The same cannot be done for λE, because the jump in the middle of the flux profile between flight level T2 and $\sim$T2 is too large to perform a reliable linear extrapolation to the ground. The results show that the other factors, like flux-loss associated to airborne eddy-covariance or transient effects, may be more important than the divergence term in deep midday CBLs.

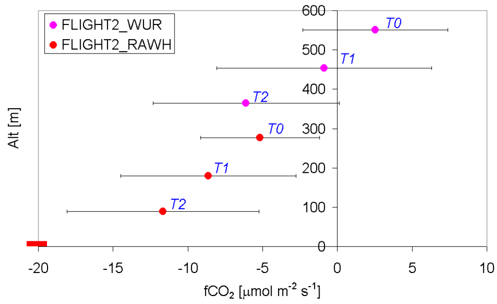

Fig. 5. Carbon-dioxide flux at different altitudes (circles) from flux-divergence flight no. 2 and 3 and its observed range at ground-site ’Marmande’ during flight time (rectangular box). Observations of both aircrafts are merged (purple = I-RAWH; red = PH-WUR). Time stamps are reported on each flight legs.

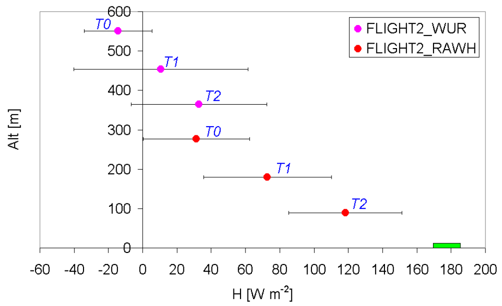

Fig. 6. Same as Fig. 5, but now for sensible heat flux (H).

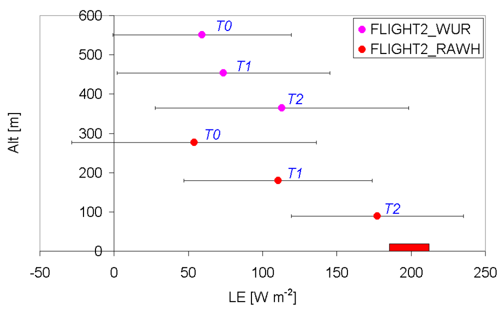

Fig. 7. Same as Fig. 5, but now for latent heat flux (LE).

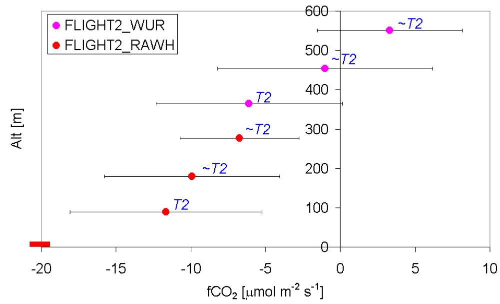

Fig. 8. Same as Fig. 5, but now with empirical corrections applied.

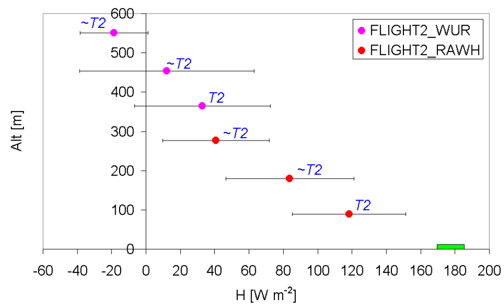

Fig. 9. Same as Fig. 5, but now sensible heat flux (H) with empirical corrections applied.

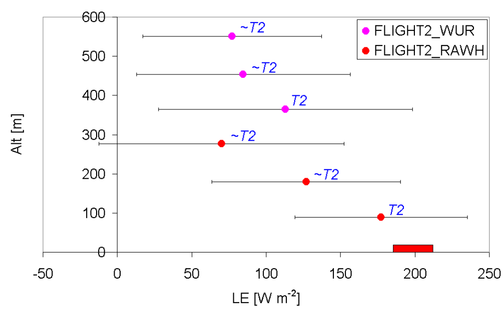

Fig. 10. Same as Fig. 5, but now latent heat flux (LE) with empirical corrections applied.

3.4 Conclusion

When dealing with flux measurements taken at a height of about 82 m above ground, which was the object of the study in the main article, a possible underestimation of surface fluxes may occur, which is in part contributed by vertical flux divergence, and in part by flux-loss associated to airborne eddy covariance or by transient effects. The results from our flux-divergence flights show that the latter two may be more important than the divergence term in deep midday convective boundary-layers, also because the maximum CBL-depth observed during this experiment was approx. 600 m, which is lower than depths observed during both periods studied in the main article.

References

Bange, J., Zittel, P., Spiess, T., Uhlenbrock, J., and Beyrich, F.: A new method for the determination of area-averaged turbulent surface fluxes from low-level flights using inverse models, Boundary-Layer Meteorology, 119 (3), 527–561, 2006.

Mahrt, L.: Surface heterogeneity and vertical structure of the boundary layer, Boundary-Layer Meteorology, 96 (1–2), 33–62, 2000.

Shuttleworth, W.J.: Macrohydrology - the New Challenge for Process Hydrology, Journal of Hydrology, 100 (1–3), 31–56, 1988.

Wood, N., and Mason, P.: The Influence of Static Stability on the Effective Roughness Lengths for Momentum and Heat-Transfer, Quarterly Journal of the Royal Meteorological Society, 117 (501), 1025–1056, 1991.